Satellite Synthetic Aperture Radar Detection of Ocean Internal Waves in the South China Sea

PI: Quanan Zheng
Department of Atmospheric and Oceanic Science, University of Maryland, College Park, MD 20742
Tel.: (301) 405-8253 Fax: (301) 314-9482 e-mail: quanan@atmos.umd.edu

CO-PI: R. Dwi Susanto
Lamont Doherty Earth Observatory of Columbia University, Palisades, NY10964-8000
Tel.: 845-365-8545 Fax: 845-365-8157 e-mail: dwi@ldeo.columbia.edu

Grant Number: N00014-05-1-0328

LONG-TERM GOALS

The long-term goal of the project is to meet the goal of ONR DRI NLIW, which is to achieve the basic science understanding that leads to a predictive capability that will be able to tell when and where non-linear internal waves will occur and what effects they will have on the hydrodynamic and acoustic environment. This project focuses on the use of remotely sensed variables, together with models, that can reproduce and predict the generation and structure of these waves, their evolution during propagation, and the processes controlling dissipation.

OBJECTIVES

1) To determine the statistical features of ocean internal waves in SCS. Interpreting ten years of satellite synthetic aperture radar (SAR) images, the statistical features of ocean internal waves in SCS will be determined. The statistical items will include the wavelength distribution, distribution of number of waves in a wave packet, characteristic half width distribution, generation location distribution, occurrence seasonal distribution, and propagation direction spectrum on the continental shelf. The statistical analysis includes the ocean environment conditions and its seasonal variability. The results will provide the users an outline of internal wave behavior in SCS, serve as a basis for empirical prediction of internal wave behavior in SCS, and contribute to creation of a predictive system.

2) To understand the effects of topography/thermocline on the evolution of solitary internal waves in SCS. Sharp changes in bottom topography and thermocline depth are an obvious feature of the SCS continental shelves. Combining satellite images, field observations, and solitary wave dynamics, the effects of those boundary conditions on the evolution of the internal solitons will be examined. The results may be used to predict the behavior of internal waves propagating over the shelf slope.

3) To explore the SAR imaging conversion mechanisms of internal waves. On the basis of the physics of radar imaging of ocean processes, the mechanisms for polarity conversion (bright-dark) of internal waves SAR image will be examined. The results will further reveal SAR imaging mechanisms and be used for SAR image interpretation.

Report Documentation Page

Form Approved
OMB No. 0704-0188

1. REPORT DATE	2. REPORT TYPE	3. DATES COVERED
30 SEP 2006		**00-00-2006 to 00-00-2006**

4. TITLE AND SUBTITLE	5a. CONTRACT NUMBER
Satellite Synthetic Aperture Radar Detection of Ocean Internal Waves in the South China Sea	5b. GRANT NUMBER
	5c. PROGRAM ELEMENT NUMBER
6. AUTHOR(S)	5d. PROJECT NUMBER
	5e. TASK NUMBER
	5f. WORK UNIT NUMBER
7. PERFORMING ORGANIZATION NAME(S) AND ADDRESS(ES) **University of Maryland, College Park,Department of Atmospheric and Oceanic Science,College Park,MD,20742**	8. PERFORMING ORGANIZATION REPORT NUMBER
9. SPONSORING/MONITORING AGENCY NAME(S) AND ADDRESS(ES)	10. SPONSOR/MONITOR'S ACRONYM(S)
	11. SPONSOR/MONITOR'S REPORT NUMBER(S)

12. DISTRIBUTION/AVAILABILITY STATEMENT
Approved for public release; distribution unlimited

13. SUPPLEMENTARY NOTES

14. ABSTRACT

15. SUBJECT TERMS

16. SECURITY CLASSIFICATION OF:			17. LIMITATION OF ABSTRACT	18. NUMBER OF PAGES	19a. NAME OF RESPONSIBLE PERSON
a. REPORT **unclassified**	b. ABSTRACT **unclassified**	c. THIS PAGE **unclassified**	**Same as Report (SAR)**	**8**	

APPROACH

1) Satellite images and field data. Satellite SAR is the most powerful sensor for ocean remote sensing because of its all weather, all day abilities, and high spatial resolution. The spatial resolution of the state-of-the-art satellite SAR images reaches 20 – 30 m, and the swath width reaches 100 – 450 km. These specifications match the requirements for observing the ocean internal waves with a spatial characteristic scale within a range from 0.1 km to 10 km. The SAR images used for the project were taken by the ERS-1 and 2, the RADARSAT-1 and 2 satellites. Historical AXBT data will be used to determine the vertical thermal structure in the study area. The data will be obtained from NOAA archives, which are in the public domain.

2) Data processing methods. Commercialized image processing software packets will be used for imagery enhancement, orthorectification, filtering, and data extraction.

3) Theoretical analysis. The objectives of theoretical analysis are to understand the nature, physics, mechanism, and laws of variation of the studied process, to derive unknown geophysical parameters using parameters and information derived from SAR image interpretation as inputs, to analyze the relation between the studied process and the surrounding environment, and to predict the future development of the studied process.

Dr. Quanan Zheng serves as a lead PI and coordinates the project. Zheng will focus on data collection, satellite image interpretation, and the theoretical analysis. Dr. R. Dwi Susanto from LDEO, Columbia University, serves as a Co-PI. Susanto focuses on image processing, statistical analysis, and takes part in data collection and the theoretical analysis.

WORK COMPLETED

1) Statistical analysis. The statistical analysis of IW occurrence in the northern South China Sea (NSCS) has been completed using seven years of satellite SAR images from 1995 to 2001. The statistical analysis of sea surface boundary conditions has been completed using long-term field measurements of sea surface wind and sea state in NSCS[Editorial Group, 1982]. The statistical analysis of IW generation boundary conditions in the Luzon Strait has been completed using 20 years of vertical temperature profiles from 1980 to 1999 [Boyer and Levitus, 1994].

2) Dynamical analysis. Nonlinear analysis of effects of shoaling thermocline on the IW generation has been completed. The role of Kuroshio playing in IW generation in the Luzon Strait has been analyzed using linear wave models and the Fourier transform methods. Dynamical analysis of bottom-topography-induced stationary IW in NSCS has been completed.

3) Paper preparation. Based on the results, six papers (see **PUBLICATIONS**) have been prepared and submitted to international-circulated and peel-reviewed journals. Three of them are accepted and in press.

RESULTS

1) Statistics of IW occurrence in NSCS. Using seven years of satellite SAR images from 1995 to 2001, statistics of IW occurrence in NSCS generate the following results.

Latitudinal distribution of IW packets in NSCS is shown in Figure 1 (partially from Zhao et al., 2004).. Statistics indicate that 22% of IW packets distributed in the east of 118ºE obviously originate from the Luzon Strait, and 78% of IW packets west of 118ºE may propagate from the east or evolve from the solitons originating from the east boundary owing to the fission effect of shoaling thermocline.

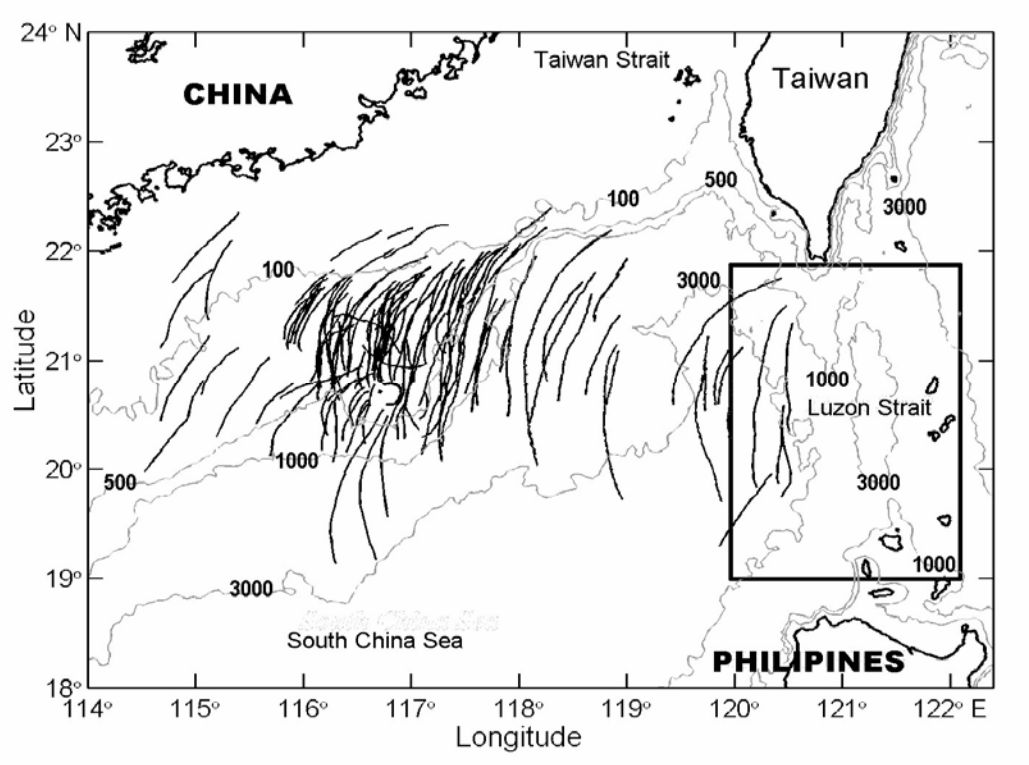

Figure 1. A map of latitudinal distribution of IW packets in NSCS. Bold lines represent crest lines of leading waves in IW packets interpreted fro*m *SAR images. The rectangular box on the right defines an IW generation source region for the dynamical analysis.

Yearly distribution of IW occurrence frequencies is shown in Figure 2. One can see an interannual variability, the frequencies in 1995, 1998, and 2000 are 2 to 5 times higher than that in other years. This interannual variability implies that there are long-term and large scale processes modifying the SAR-observed IW occurrence.

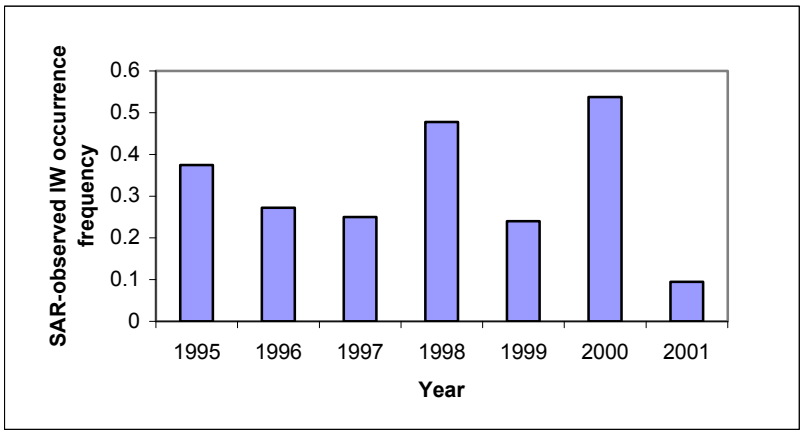

Figure 2. Yearly distribution of SAR-observed IW occurrence frequencies in NSCS.

M**onthly SAR-observed IW occurrence frequencies** show that the high frequencies are distributed from April to July and reach a peak in June with a maximum frequency of 20%. The low occurrence frequencies are distributed in winter from December to February of next year with a minimum frequency of 1.5% in February (Figure 3).

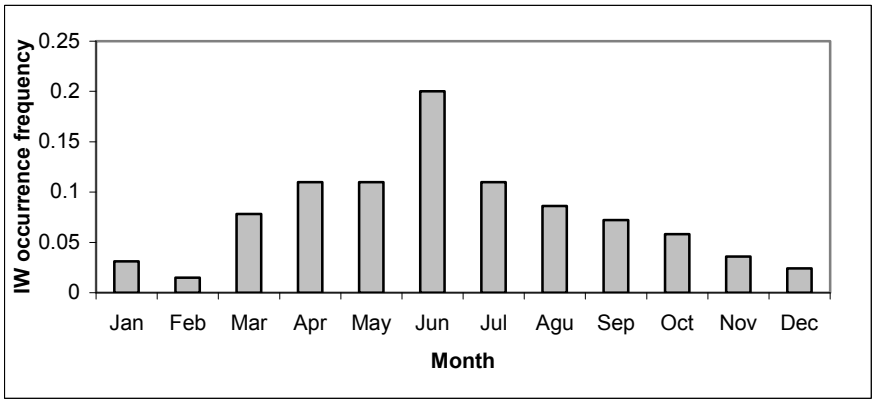

Figure 3. Monthly distribution of SAR-observed IW occurrence frequencies in NSCS.

2) Statistics of sea surface boundary conditions. Statistics indicate that high frequencies of low wind conditions (scales 0-1 and 2-3) are distributed from April to September and reach a peak phase from May to July with a maximum frequency of 58% in July. The low frequencies are distributed from November to March of next year. The frequency distributions of high wind conditions (scales 4-5, 6-7, and 8) are just anti-phase with low wind conditions. High frequencies are distributed from October to March of next year and reach a peak phase from November to January with a maximum frequency of 87% in December (Figure 4).

The statistical distribution of monthly sea state frequencies is shown in Figure 5. One can see that high frequencies of Wind Wave Scales 0-2 (for the wave height less than 0.7 m) are distributed from April to August and reach a peak value of 44% in August. The low frequencies are distributed from October to February of next year with frequencies lower than 16%. March and September appear as transit

phases. The frequencies of Scales 3-4 (for the wave height from 0.8 to 1.9 m) have an almost even distribution with a mean of 41.8% and a standard deviation of 2.5%. The distributions of Scales 5 (for the wave height from 2.0 to 3.4 m) and 6 (for the wave height from 3.5 to 6.0 m) are anti-phase with Scales 0-2.

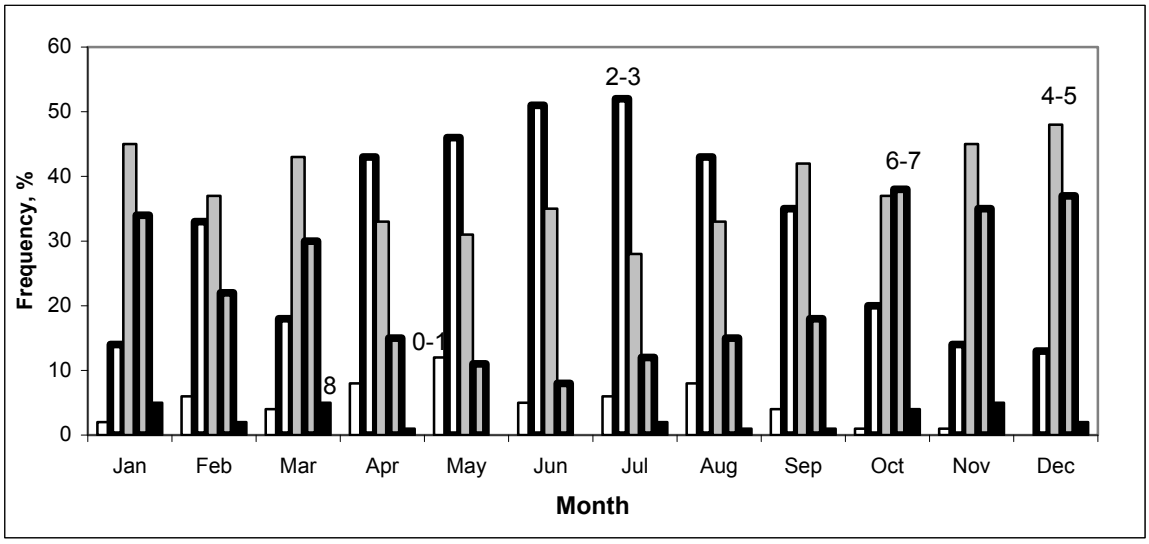

Figure 4. Statistical distributions of monthly mean wind frequencies at statistical cells centered at 22ºN 118ºE in NSCS. The numerals marked at peak bars represent wind scale ranges.

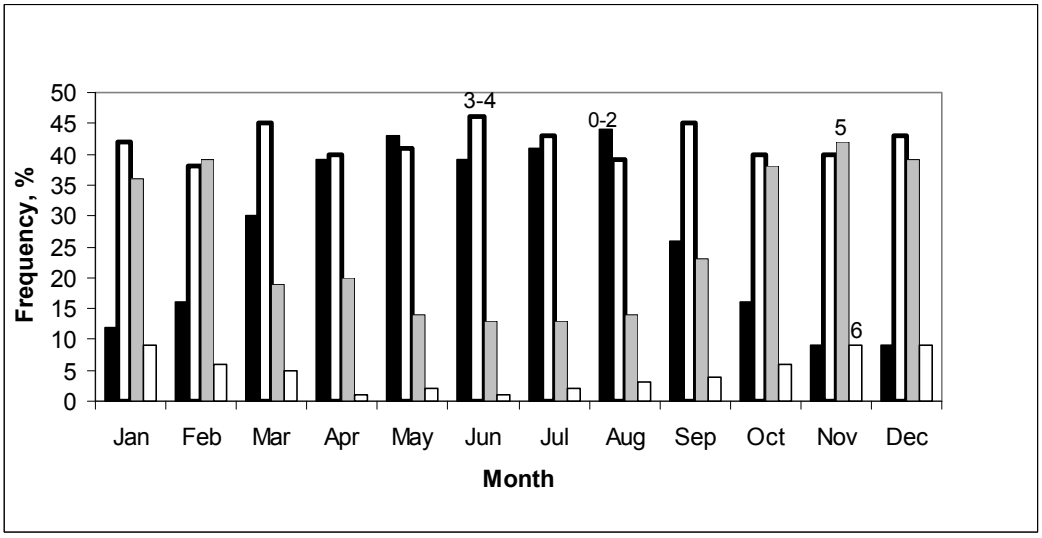

Figure 5. Same as Figure 4, but for monthly mean sea state.

3) Nonlinear analysis of effects of shoaling thermocline on the IW generation. The study proposes that the IW generation needs the necessary and sufficient conditions: initial disturbance formation, and wave amplitude growth. Due to dissipation effect on the disturbance energy, only fully grown waves have a chance to radiate out of the source region. A physical model and PKdV equation are applied to the analysis of the sufficient conditions for solitary IW amplitude growth. The results indicate that the

thermocline shoaling provides the forcing to soliton amplitude growth, so that the soliton amplitude growth ratio (SAGR) serves as a decisive factor for the IW occurrence frequency. Theoretical analysis predicts a linear relation between the two. Application of theoretical models to field measurements gives a correlation coefficient as high as 0.845 with a confidence level of 99% for months from March to November. The linear regression gives a correlation coefficient (R2) of 0.6519 and a SAGR threshold (minimum) value of 0.90 for IW occurrence. According to the theoretical solutions, the eastward propagating disturbances have no chance to grow up, so that they hardly appear in the eastern Luzon Strait.

4) The role of Kuroshio playing in IW generation in the Luzon Strait. A linear model describing western boundary current instability generation mechanism for the ocean internal waves is developed. Analytical solutions are derived from a zero-order complex frequency – wave number relation. The imaginary part gives an exponential growth rate of IW in the form of $\alpha = \sqrt{gk}\left[\left(f + \partial V / \partial x\right) / 2\partial V / \partial z\right]^{1/2}$, in which k is the wavenumber of IW, g is the gravitational acceleration, f is the Colorist parameter, and V is the meridional component of western boundary current. One can see that the internal waves would absorb the energy from the western boundary current and then grow. The real part of the relation represents a dispersion relation of the generated internal waves in the form of $\omega = \sqrt{gk}\left[\left(f + \partial V / \partial x\right) / 2\partial V / \partial z\right]^{1/2}$, in which ω is the wavenumber of IW. A significant feature of this dispersion relation is that the wave propagation characteristics are closely associated with the instability of western boundary current. The theoretical results are used in the case of the Kuroshio east of the Luzon Strait. Based on the analysis, it is found that for the western propagating disturbance, the Kuroshio west wing is unstable and the east wing is stable; while the reverse is true for the eastern propagating disturbance. The results are used to interpret satellite SAR images of the ocean internal waves, which are generated in the Luzon Strait and propagated westward.

5) Dynamical analysis of bottom-topography-induced stationary IW in NSCS. The satellite SAR images display wave-like patterns of the ocean bottom topographic features at the south outlet of Taiwan Strait (TS). Field measurements indicate that the most TS water body is vertically stratified. In order to explore the mechanisms and to determine the relations between the SAR imagery and the bottom features, a two-dimensional, three-layer ocean model with sinusoidal bottom topographic features is developed. Analytical solutions and inferences of the momentum equations of the ocean model lead to the following solutions. 1). In the lower layer, the topography-induced waves (topographic waves) exist in the form of stationary waves, which satisfy a lower boundary resonance condition σ = kC0, here σ is an angular frequency of the stationary waves, k is a wavenumber of bottom topographic corrugation, and C0 is a background current speed. 2). As internal waves, the topographic waves may propagate vertically to the upper layer with an unchanged wavenumber k, if a frequency relation $N_3 < \sigma < N_2$ is satisfied, here N2 and N3 are the Brunt-Wäisälä frequencies of middle layer and upper layer, respectively. 3). The topographic waves are extremely amplified if an upper layer resonance condition is satisfied. The theoretical SAR image of topographic waves is derived on the basis of current-modulated small wave spectra. The results indicate that the topographic waves on SAR images have the same wavelength of bottom topographic corrugation, and the imagery brightness peaks are either inphase or antiphase with respect to the topographic corrugation, depending on a sign of a coupling factor. These theoretical predictions are verified by field observations. The results provide a physical basis for quantitative interpretation of SAR images of bottom topographic waves in the stratified ocean.

IMPACT/APPLICATIONS

The results of this project will provide the users a statistical outline of internal wave behavior and boundary conditions in SCS, and will benefit the broader oceanographic community, ocean engineering industries, underwater navigation and operational users. The results may also serve as a basis for empirical, theoretical, and numerical prediction models of internal wave behavior in SCS, and contribute to creation of a predictive system. The results will further reveal SAR imaging mechanisms and be used for SAR image interpretation.

RELATED PROJECTS

The PI of this project serves as a CO-PI for an ongoing ONR PO project titled "Analysis of Fine Structures of Flows, Hydrography, and Fronts in Taiwan Strait". The study areas of two projects are immediately adjacent. Therefore, two projects sometimes share the same data resources of field observations.

REFERENCES

Boyer, T., and S. Levites, Quality control and processing of historical oceanographic temperature, salinity, and oxygen data, *NOAA Technical Report NESDIS 81*, Washington, D.C., pp. 1-64, 1994.

Editorial Group of Marine Climate Atlas of Institute of Geography, Chinese Academy of Sciences and Publishing & Compilation Group of Institute of Marine Scientific and Technological Information, National Bureau of Oceanography, China, *Climatic Atlas of Chinese Offshore Areas and Northwest Pacific,* Vol. 1, *Wind, Wave and Storm*, Ocean Press, Beijing, pp. 65 – 115, 1982.

Zhao, Z., V. Klemas, Q. Zheng, and X.-H. Yan, Remote sensing evidence for baroclinic tide origin of internal solitary waves in the northeastern South China Sea, *Geophys. Res. Lett.,* 31, L06302, doi:10.1029/2003GL019077, 2004.

PUBLICATIONS

Zheng, Q., R. D. Susanto, C-R. Ho, Y. T. Song, and Q. Xu, Statistical and dynamical analyses of generation mechanisms of solitary internal waves in the northern South China Sea. *J. Geophys. Res.,* 2006.

Zheng, Q., L. Li, X. Guo, Y. Ge, D. Zhu, and C. Li, SAR Imaging and hydrodynamic analysis of ocean bottom topographic waves. *J. Geophys. Res.,* 2006 [in press].

Susanto, R. D., L. Mitnik, and Q. Zheng, Ocean internal waves observed in the Lombok Strait. *J. Oceanogr.,* 2006 [in press].

Yuan, Y., Q. Zheng, D. Dai, F. Qiao, and J. Meng, The mechanism of internal waves in the Luzon Strait. *J. Geophys. Res.,* 2006 [in press].

Ho, C.-R., C.-Y. Lin, N.-J. Kuo, and Q. Zheng, Analyses of upper layer thickness variation in the South China Sea from satellite altimeter data and in situ measurements. *Rem. Sens. Environ.,* 2006.

Hong, H., J. Hu, Z. Chen, Q. Zheng, and C. Li, Three-dimensional structure of a low salinity tongue in the southern Taiwan Strait observed in summer 2005. *Geophys. Res. Lett.,* 2006.